

## Performance Improvement of a Single Phase Induction Motor Fed by Nonsinusoidal Voltages

Dr. Jamal A. Mohammed \*

Received on: 17/12/2006

Accepted on: 3/4/2008

### Abstract

The distorted voltage waveforms, which have, more or less, a high harmonic content, have negative impact on the long-term performance of the motor, as they cause nonsinusoidal currents in the stator and the rotor, and consequently additional losses and distorted torque in the machine.

The steady state performance of Permanent Capacitor single phase induction motor fed by optimal SHEPWM inverter is studied with respect to harmonics, additional losses and torque pulsations. The effectiveness of the optimal SHPWM technique in improving of motor performance is investigated analytically.

**Key-Words:** Nonsinusoidal, single phase induction motor, SHEPWM.

الخلاصة

" " " " "

"

"

### I. Introduction

Single phase AC induction motors are one of the most widely used motors in the world, especially for domestic or commercial applications where a three phase power supply is not available [1].

It is well known that nonsinusoidal power supply can cause several harmful effects on induction motor such as rotor vibration, extra

losses and excessive temperature rise [2]. Thus motor may become noisy when fed by a nonsinusoidal source such as voltage source inverters (VSIs), so it is important to study this phenomenon.

Many contributions can be found in the bibliography concerning the induction motor behavior under nonsinusoidal stator voltages [2,3,4]. Therefore, it is necessary to use an optimum technique that improves the

\* Dept. of Electromechanical Engi., Univ. of Tech.

motor performance and makes it quieter [5,6]. The work [7] proposed a new method to get optimal solutions using Selective Harmonic Elimination PWM SHEPWM technique. Figure 1 shows the optimal SHEPWM scheme.

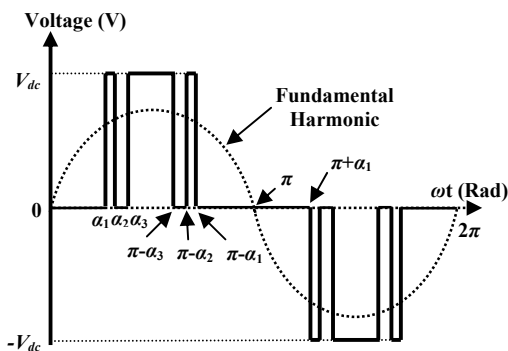


Fig. 1: Optimal SHEPWM Switching Scheme

In the present work the operation of a Permanent Capacitor single phase induction motor fed through optimal SHEPWM inverter is analyzed. The simulation of the proposed motor is carried out by using equivalent circuit model, where the stator voltages are sum of a number of sinusoidal components with frequencies multiple of the fundamental harmonic. The terms of this sum can be derived from Fourier analysis of any given voltage waveform.

**II. Theory of the Motor**

Most single phase motors are constructed with two windings which are physically displaced 90° around the motor stator. The windings are often asymmetrical, in which case the "main" winding will have a higher current rating. Furthermore, the "auxiliary" winding is connected to the AC supply through a series capacitor, as shown in Figure 2, to make its current lead the

main winding current by approximately 90° in phase [1].

Permanent Capacitor single phase induction motor produces approximation of two phase operation at the rated point. This results in better efficiency and power factor and lower (2f) torque pulsations than in equivalent Capacitor-start and Split-phase design. Such motor will have a perfectly uniform rotating magnetic field at some specific load and it will behave just like a two phase induction motors at that point.

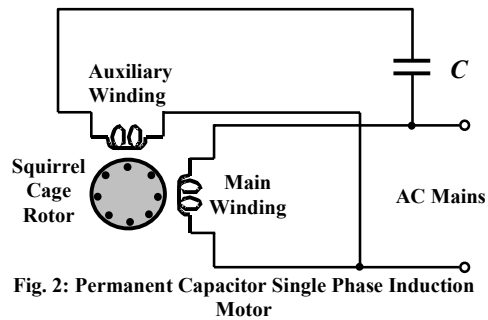


Fig. 2: Permanent Capacitor Single Phase Induction Motor

The present work will use the revolving field theory for studying the performance of the single phase Permanent Capacitor induction motor fed by SHEPWM inverter.

This theory basically states that a stationary pulsating magnetic field can be resolved in two rotating magnetic fields, each of equal magnitude but rotating in opposite directions. The induction motor responds to each magnetic field separately, and the net torque in the machine will be the vector sum of the torque due to each of the two magnetic fields [8].

Single winding single phase motors are most effectively analyzed using the Double Revolving, Field theory, which splits the oscillating

single magnetic field produced by a current flowing through the winding into two contra-rotating magnetic fields, each of which can be analyzed using normal three phase rotating field theory. The equivalent circuit for a single winding motor under these conditions is shown in Figure 3 [9].

The rotor impedance referred to the stator has been separated into two halves, with one half influenced by the forward rotating field and the other influenced by the backward rotating field.

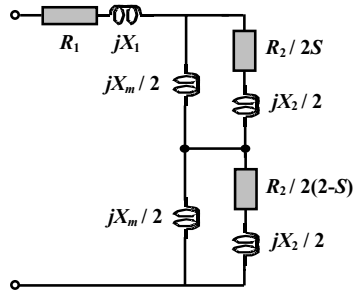


Fig. 3: Equivalent Circuit of Single Winding Single Phase Induction Motor

For a two winding motor, with the windings arranged in space quadrature on the stator, this analysis can be extended to develop a similar single phase equivalent circuit for each winding, with an additional speed voltage in each winding representing the voltage induced in the winding from the other winding's flux. The total equivalent circuit for this arrangement is shown in Figure 4, for two unbalanced windings with a turn's ratio of " $1/a_s = N_a / N_m$ " between the main and the auxiliary winding. Note that the parallel branches for each winding equivalent circuit have been converted into equivalent series impedances [9,10].

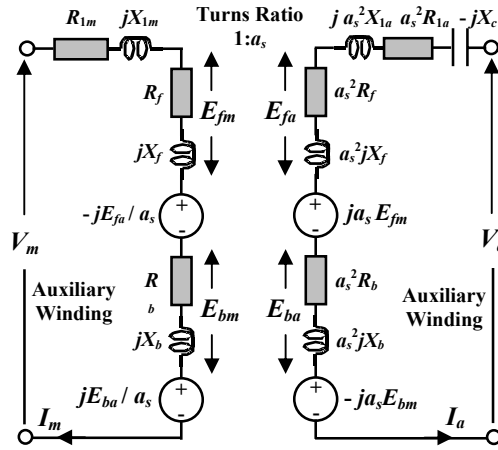


Fig. 4: Equivalent Circuit of Unbalanced Two Winding Induction Motor

### III. Steady-state Equivalent Circuits

Although single phase induction motor drives have relatively simple construction, they are more difficult to analyze than three phase motors because of the unbalance stator winding. The steady-state equivalent circuits of the Permanent Capacitor motor in terms of positive and negative sequence variables, forward and backward components, and the resultant electric torque expressions were developed as in the Ref. [9]. The necessary equations are listed in the Appendix A.

### IV. Motor Analysis on Nonsinusoidal Voltages

The method of analysis of performance of induction motor operating on nonsinusoidal input waveforms obtained by the following ways:

1. The input wave is resolved into Fourier series.
2. Direct solution of machine equations for given input waveform. This is done

using analogue or digital simulation. The well known numerical methods are used for the solution of the machine equations.

**A. Steady State Analysis Using Fourier Series**

There is an amenable for the analysis of the inverter output voltage waveforms using Fourier series. The voltage waveform contains odd harmonics and does not contain even harmonics. Using Fourier series a general expression can be written for the voltage applied to the motor as:

$$V_{ins} = \sqrt{2} \left[ V_1 \sin \omega t + V_3 \sin 3\omega t + V_5 \sin 5\omega t + \dots \right] \quad (1)$$

where  $V_1$  is the fundamental voltage, and  $V_3, V_5, \dots$  are the harmonic voltages.

Assuming no saturation, principle of superposition can be applied to determine the overall performance of the induction motor on non-sinusoidal voltages. The motor behavior for fundamental as well as for each harmonic is determined independently. These individual responses are added up to obtain overall performance. In other words, the net current and torque of the motor are equal to the sum of the current and torque contributions of each harmonic (voltage) of the voltage waveform. The conventional equivalent circuit is used in the analysis. The behavior of the motor for a harmonic voltage is obtained by suitably modifying the equivalent circuits; one for each harmonic is used to calculate the complete steady-state behavior of the motor.

**B. Harmonic Equivalent Circuits**

The equivalent circuit for a Permanent Capacitor single phase induction motor is shown in Figure 3. The core loss and core loss current are neglected,  $S_1$  is the slip for the fundamental and it is given by:

$$S_1 = (N_s - N_r) / N_s \quad (2)$$

where  $N_s$  and  $N_r$  are the synchronous and rotor speeds respectively. The harmonic voltages applied to the motor produce harmonic currents. These currents in turn produce rotating *mmf's*. These *mmf's* have a speed which is a multiple of the harmonic order and fundamental synchronous speed. Certain *mmf's* rotate in the forward direction and certain others rotate in the back word direction. Thus the speed of the  $n^{th}$  harmonic *mmf* is  $nN_s$ . The slip for the  $n^{th}$  harmonic is in general:

$$S_n = (nN_s \pm N_r) / nN_s \quad (3)$$

Use the negative sign, if the harmonic rotates in the forward direction and the positive sign, if the harmonic rotates in the backward direction.

The spectrum of harmonic currents is known, from which the total harmonic content can be obtained as:

$$I_h = \sqrt{I_3^2 + I_5^2 + I_7^2 + \dots} \quad (4)$$

and the *rms* value of the current is:

$$I = \sqrt{I_1^2 + I_h^2} \quad (5)$$

where  $I_1$  is the fundamental current and ( $I_3, I_5, I_7 \dots$ ) are the harmonic currents. The fundamental current  $I_1$  depends upon the slip or load whereas  $I_3, I_5, \dots$  are almost independent of load. This is

because the slip for any harmonic field is almost unity due to very small value of fundamental slip. As the load increases, the harmonic content decreases in relation to the fundamental [13].

The instantaneous torque can be calculated from Eq. A.6 in the Appendix A. The time variation of the torque can be found to contain a steady and pulsating torque.

The torque resulting from reaction of the harmonics of different orders in the stator gives rise to pulsating torque whose average value is zero. Fourth harmonic torque pulsations due to reaction of the fundamental of stator and 3<sup>rd</sup> harmonics of the rotor currents, or the 3<sup>rd</sup> harmonics of stator and 7<sup>th</sup> harmonics of the rotor currents, and so on.

#### **V. Motor Parasitic Torque Due to Nonsinusoidal Voltages**

It has been shown that the output voltage of PWM power inverters exhibits harmonic distortion due to several causes: the modulation algorithm, nonlinearities in the output filters, dead times, voltage drop across the switches and modulation of the DC bus voltages. As a result, motors driven by these inverters have important torque pulsations [5].

A torque is developed due to interaction between forward and backward of stator and rotor *mmf*'s having the same number of poles. When a stator winding of  $(2P)$  poles of an induction motor is excited by a single phase system of frequency  $n f_1$ , ( $n = 0, 1, 3, 5...$ ), stator magnetic field is developed which rotates at speed of  $n N_s$  relative to stator.

The torques developed by the field of different speed pulsate with a frequency corresponding to the difference of the speeds of rotor and stator *mmf*s. The *mmf*s have the same number of poles. So each stator *mmf* reacts with other rotor *mmf* to produce a torque. For a chosen order  $n$ , there are  $(n.n)$  torques:

1. Useful torque:  $n_1 = n_2 = 1$ .

2. Parasitic torques:

a.  $n_1 = n_2 > 1$ :  $(n-1)$  torques due to the interaction of stator and rotor *mmf*s harmonic of same order. These are steady synchronous torques. Both braking and motoring torques are possible. These are normally very small in the inverter operation of the motor and can be neglected.

b.  $n_1 \neq n_2$ :  $n(n-1)$  torques due the interaction of stator and rotor *mmf*'s harmonics of different order. These are called "pulsating torques".

The amplitude of pulsations depends upon the harmonic content of the voltage waveform. The lower order harmonic torque pulsations may become objectionable at smaller speed of operation. Therefore these have to be made as small as possible. This is done by increasing the number of switching of the inverter fed to the motor. Another way of controlling the amplitude of pulsations depends upon the type of control strategy [11,12].

#### **VI. Motor Operation on Nonsinusoidal Voltages**

The performance of the motor depends upon the type of inverter, and then the discussion of the behavior of the motor is given with respect to harmonics and torque pulsations. The voltage waveform depends solely on the

conduction of the switch device and is independent of load.

Fourier analysis of the waveform is given as in Eq. 1. Besides the fundamental, the voltage harmonics present of order  $n = 2k+1$  (when  $k=1, 2, 3\dots$ ) are:

$$V_n = V_1 / n \quad (6)$$

### **VII. Additional Losses in the Motor**

When induction motors are connected to a distorted supply voltage, their losses increase due to the time harmonics. These losses can be classified into four groups:

1. Losses in the stator and rotor conductors, known as copper losses.
2. Losses in the terminal sections, due to harmonic dispersion flows.
3. Losses in the iron core, including hysteresis and Foucault effects; these increases with the order of the harmonic involved and can reach significant values.
4. Losses in the air gap. The pulsating harmonic torques are produced by the interaction of the flux in the air gap with the rotor harmonic currents, causing an increase in the energy consumed [12,13].

These increased losses reduce the motor's life. The effect of the copper losses intensified in the presence of high frequency harmonics, which augment the skin effect, reducing the conductors' effective section and so increasing their physical resistance. Additional losses can be summarized as follows:

#### **A. Additional Copper Losses**

These are influenced by the harmonics content of the stator and rotor currents. At higher harmonics the

increase in the resistance due to (skin effect) must be only considered. The additional copper losses are determined by adding the losses due to each harmonic. The increase in the stator copper losses is given by:

$$P_{Cu_s} = \sum_n I_{m_n}^2 R_{1m} + I_{a_n}^2 R_{1a} \quad (7)$$

where  $I_{m_n}$  and  $I_{a_n}$  is the main and auxiliary harmonic currents respectively.

In the stator, the skin effect is very small. Taking into consideration various factors that influence stator resistance, the above equation describes the losses exactly. The increase in the rotor copper loss is given by:

$$P_{Cu_r} = \sum_n I_{r_n}^2 R_2 = \sum_n S_n T_{av_n} \quad (8)$$

where  $I_{r_n}$  and  $T_{av_n}$  are the rotor harmonic current and harmonic average torque respectively.

The resistance variation due to skin effect cannot be neglected in the case of squirrel cage rotors, particularly if deep bars are used. These additional rotor copper losses form a large portion of additional losses in the induction motors operating on nonsinusoidal supplies and are the main cause for reduced efficiency.

#### **B. Additional Core Losses**

The resultant waveform of the air gap flux density will not be constant around the air gap and it may be greater or less than fundamental wave. The Hysteresis, eddy currents and time harmonic fluxes decide these losses. An exact determination of these losses is rather difficult. It is very small in

comparison with the other additional losses.

### C. Additional Stray Losses

These are due to space harmonics, cross currents in iron and additional iron losses. The normal stray load losses are contributed by end leakage and skew leakage flux. These losses are normally (0.5%) of the rated output ( $P_2$ ) with sinusoidal excitation.

In general the additional losses can be decreased by reducing the harmonic content of the voltage waveform.

The optimum PWM technique should minimize additional harmonic losses in the motor [3,5,7].

The addition of all previous losses gives the total losses  $\sum P$  and efficiency ( $\eta$ ) will be:

$$\eta = P_2 / P_1 = P_2 / (P_2 + \sum P) \quad (9)$$

## VIII. Simulation Results

In this work a simulation program is developed for studying the behavior of Permanent Capacitor single-phase induction motor operated on an optimal SHEPWM inverter. Discussion of simulation results can be divided into the following procedure:

1. Calculations of the optimized switching angles ( $\alpha_1, \alpha_2, \alpha_3 \dots \alpha_7$ ) for optimal SHEPWM inverter and the corresponding harmonics voltage amplitude [7].
2. Studying the behavior of optimal SHEPWM inverter with respect to switching losses and performance factor; the Total Harmonic Distortion (THD).

3. Studying the behavior of motor operated on optimal SHEPWM inverter with respect to additional power losses and torque pulsations.

For SHPWM scheme shown in Figure 1, computation was done as the modulation index  $m$  increased between (0 and 1). The optimum calculated switching angles  $\alpha$  of this scheme is illustrated as in the Table 1. Figure 4 shows the instantaneous motor current with different number of switching angles per quarter cycle of the output waveform  $s$ . It can be seen from the figure that the ripple of current decreases with increasing of  $s$ , since increasing of  $s$  causes increase of the motor impedance with frequency ( $X=2\pi fL$ ), therefore, the harmonic current will decrease for constant harmonic voltage amplitude as shown in Figure 5. Therefore the induction motor can be represented as a good low pass filter. The voltage THD is very important in the inverter performance evaluation. Figure 6 illustrates the relationship between this factor and the modulation index  $m$  with different number of switching angles  $s$  for optimal SHEPWM scheme. Decreasing of  $m$  has direct effects, causing an increase in the harmonic amplitude [7]. This increase leads to increase the harmonic currents and torque pulsations. Increasing of harmonic currents causes increase of motor copper losses as a heat and increasing in the performance factor (THD). As a result, THD decreases with increasing  $s$ , and increase with decreasing  $m$  as shown in Figure 6.

Therefore increasing of  $s$  is the way to reduce the negative effects of reducing  $m$  when small values of voltages and

frequencies are required in the output of the inverter, especially in Adjustable Speed Drive (ASD).

We can see from Figure 7 that THD<sub>max</sub> decreases with increasing  $s$  while THD<sub>min</sub> approximately constant.

The increasing of  $s$  means more inverter switching losses [See Figure 6]. So it is very important to take switching losses into consideration.

By using the equivalent circuit of the motor shown in Figure 3 and the performance equations in the Appendix A, it can be easy to analyze the motor performance operated on a SHEPWM inverter, and using Fourier series to calculate the harmonic currents amplitude which important of studying the motor behavior.

Table 1 illustrates the values of the optimal switching angles  $\alpha$ , harmonics amplitude, output power ( $P_2$ ), input power ( $P_1$ ), additional losses ( $\Sigma P_{add}$ ), power factor ( $P_f$ ), inverter switching losses ( $P_{sw}$ ) and the overall efficiency ( $\eta$ ) for the proposed technique.

Increasing of  $s$  causes increasing of the motor impedance, therefore the harmonic currents will decrease [7]. Decreasing the harmonic currents causes decreasing of additional torque pulsations, as illustrated in Figure 6. The pulsating torque is obtained at all even multiples of supply frequency. Notice that, the additional torque pulsations decreases with increasing of  $m$ . When  $m$  increases until  $s=7$  (Elimination of 6-low order harmonics), the low order of even harmonics and multiple of torque pulsations will be suppressed, except the component of order 2, then motor will behave just like motor supplied by sinusoidal power

supply, so that the motor will be more quite with high  $s$ .

We can see from Figure 6 that, increasing  $s$  in SHPWM scheme reduces the modulation index range.

We can also see from the same figure that increasing  $s$  causes decreasing of the motor input power, power losses and additional losses and increasing of power factor and overall efficiency until the motor performance [at  $s=7$ , see Table 1] convergences from the rated values which is illustrated in the Table B.1 in the Appendix B.

Figure 7 illustrates the optimum performance of the inverter and motor fed from versus number of switching angles ( $s$ ) by using the optimal SHPWM technique.

## **IX. Conclusions and Suggestions**

The proposed motor becomes noisy when fed by nonsinusoidal supply such as voltage source inverter. It works with distorted harmonic currents, additional power losses and additional torque pulsations in the output torque from the motor shaft which cause reduction in the lifetime of the motor.

When optimal SHEPWM inverter is used in driving motor, eliminating of more low-order harmonic voltages leads to great reduction of low-order harmonic pulsation torques generated by the motor, reduction of additional power losses, improving of line power factor, minimizing of current distortion, increasing the motor efficiency, and then improving of motor performance which make the motor behave just like a quite motor supplied from pure sinusoidal excitation.

It was shown that quality factor of the performance evaluation of the

inverter (THD) vary in value with the number of eliminated harmonics and the fundamental amplitude, and decrease with their increase.

The suggestion for future work is to extend the number of switching angles more than seven to improve the performance of the motor until making its behavior exactly like one excited from pure sinusoidal supply, or change the modulation scheme without increasing the switching angles (switching losses).

It is very good to generate a variable-frequency; variable-voltage supply to get adjustable-speed drives.

## X. References

- [1] Baghzouz Y., and Tan O. T., "PWM Inverter-fed Single-phase Induction Motor Drives," *Journal of Energy System*, Vol. 8, No. 3, 1988.
- [2] Rakotonirina, G. J. Xu, A. Sevigne and P. Sicard, "Thermal Effects of Nonsinusoidal Supply on Three-Phase Induction Motor Behavior," *Electrimacs*, 2002, August, pp. 18-21.
- [3] Ching-Yin Lee, Wei-Jen Lee, "Effects of Nonsinusoidal Voltage on the Operation Performance of a Three-phase Induction Motor," *IEEE Transactions on Energy Conversion*, Vol. 14, No. 2, pp. 193-201, June 1999.
- [4] Vamvakari, A. A. Kandianis, A. Kladas, S. Manias and J. Tegopoulos, "Analysis of Supply Voltage Distortion Effects on Induction Motor Operation," *IEEE Transactions on Energy Conversion*, Vol. 16, No. 3, pp. 209-213, Sep., 2001.
- [5] Oliva, A. H. Chiacchiarini, A. Ayamono, and P. Mandolesi, "Reduction of Total Harmonic Distortion in Power Inverters," *Latin American Applied Research*, 35, pp. 89-93, 2005.
- [6] Williamson S., D. Pearson and A. M. Rugege, "Acoustic Noise and Pulsating Torques in Triac-Controlled Permanent-Split-Capacitor Fan Motor," *IEE Proc.*, Vol. 128, Pt. B, No. 4, July 1981.
- [7] Jamal A. Mohammed, "Optimum Solving SHEPWM Equations for Single-phase Inverter Using Resultant Method," To be published, *Engineering & Technology*, 2007.
- [8] Chapman, S. J. *Electric Machinery Fundamental*, Mc Graw-Hill, 3<sup>rd</sup> Edition, New York, 1999.
- [9] Holmes D.G. and Kotsopoulos, A. "Variable Speed Control of Single and Two Phase Induction Motors Using a Three Phase Voltage Source Inverter," in *Conf. Record of IEEE/IAS Ann. Meeting*, pp. 613-620, 1993.
- [10] Sen P.C., *Principles of Electric Machines and Power Electronics*, 2<sup>nd</sup> Edition, John Wiley and Sons, Inc., 1997.
- [11] Sernia P. and Walker, G.R. "Harmonic Quality of Multilevel Cascade Inverters with Random Carrier Phase Pulse Width Modulation," in *Computer Science and Electrical Eng.*, University of Brisbane, Australia, pp. 26-29, Sep. 2004.
- [12] subrahmanyam, V. *Thyristor Control of Electric Drives*, Tata McGraw-Hill Publishing Company Limited, New Delhi, 1988.
- [13] . Khomfoi, S.V. Kinnares and P. Viriya, "Investigation into Core Losses due to Harmonic Voltages in PWM fed Induction Motors", *IEEE, International Conference on Power Electronics and Drive Systems, PEDS'99*, July 1999, Hong Kong.

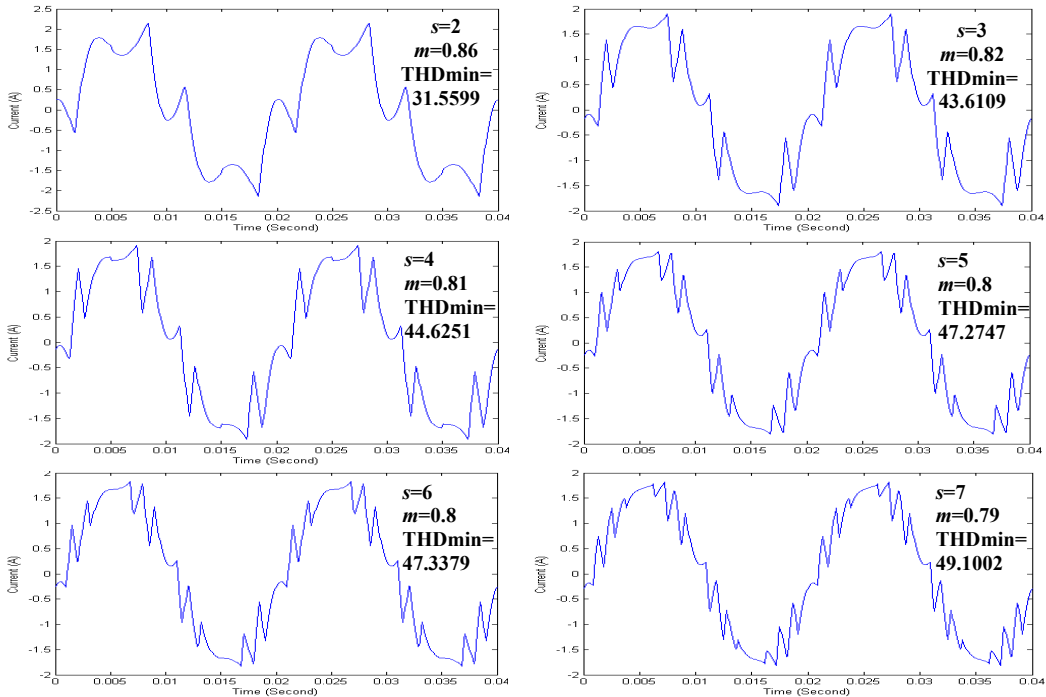


Fig. 5: Instantaneous Currents of Motor Fed by an Optimal SHEPWM Inverter for Different Switching Angles (s)

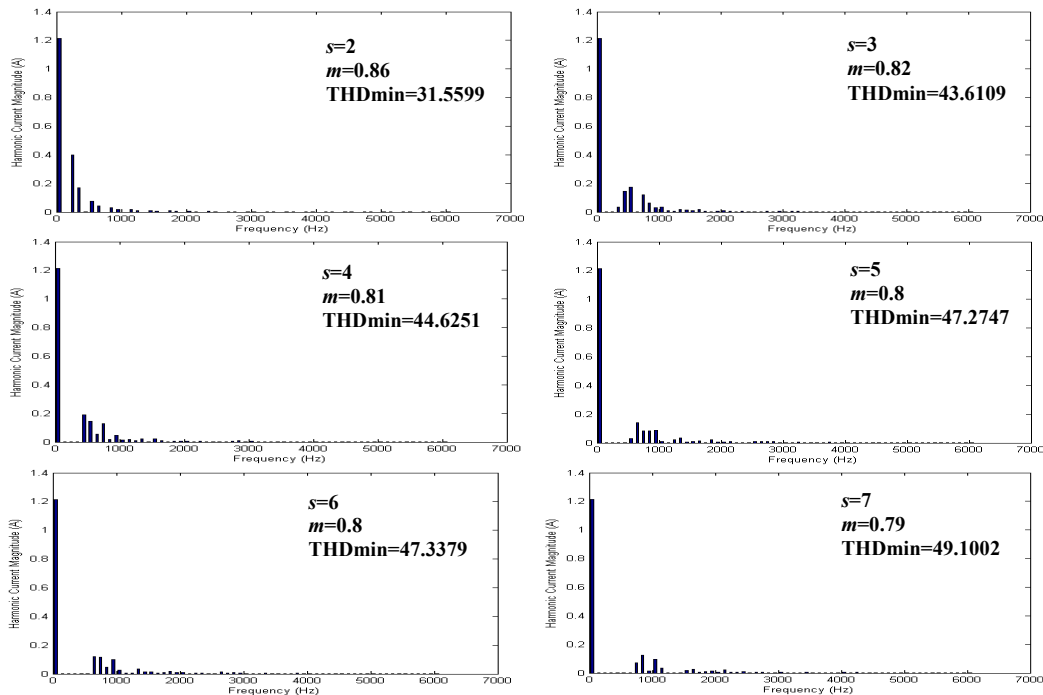


Fig. 6: Line Current Spectra of Motor Fed by an Optimal SHPWM Inverter for Different Switching Angles (s)

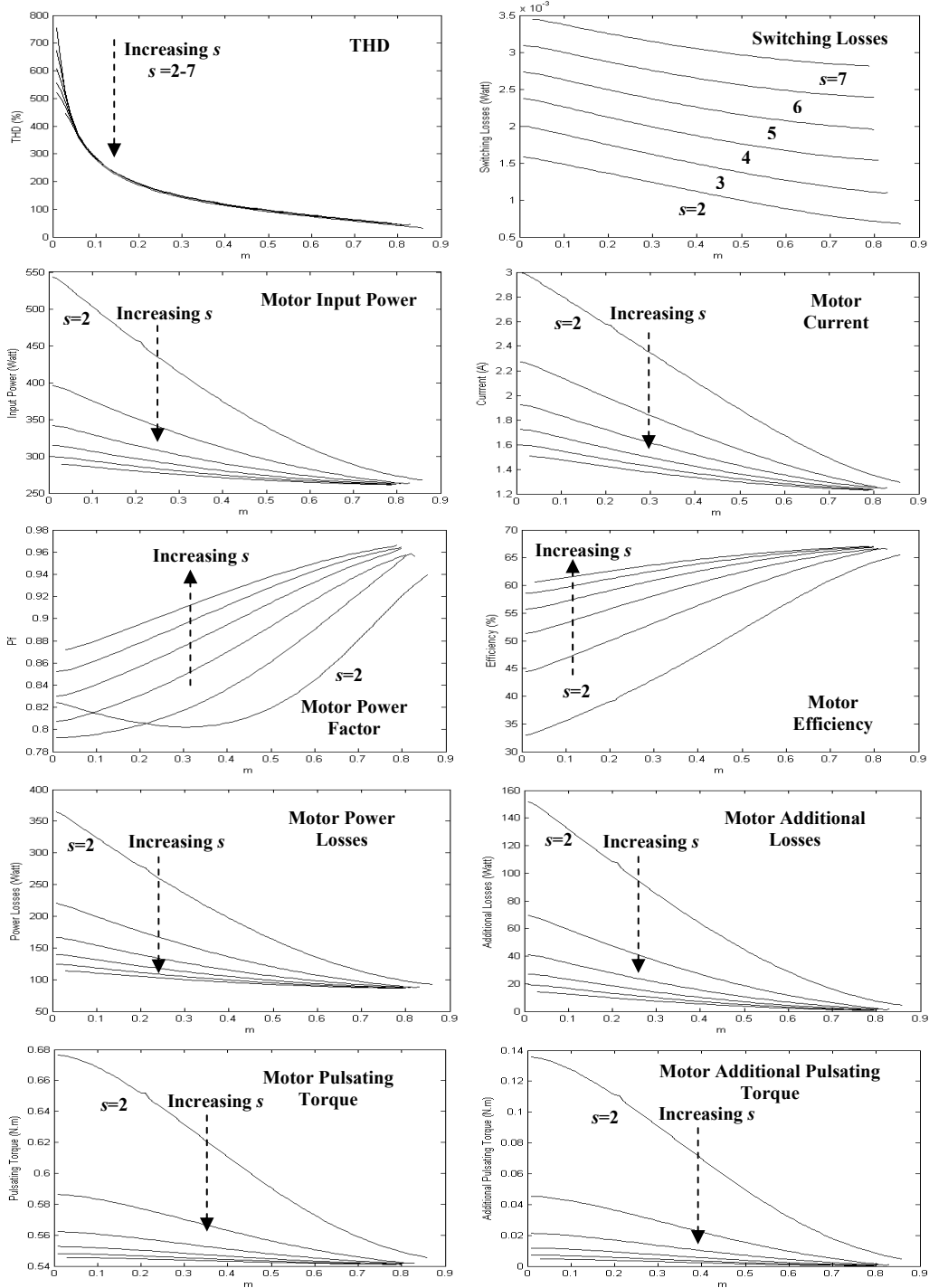


Fig7: Performance of Inverter and Motor Fed from vs.  $m$  for different  $s$  with Optimal SHPWM Technique

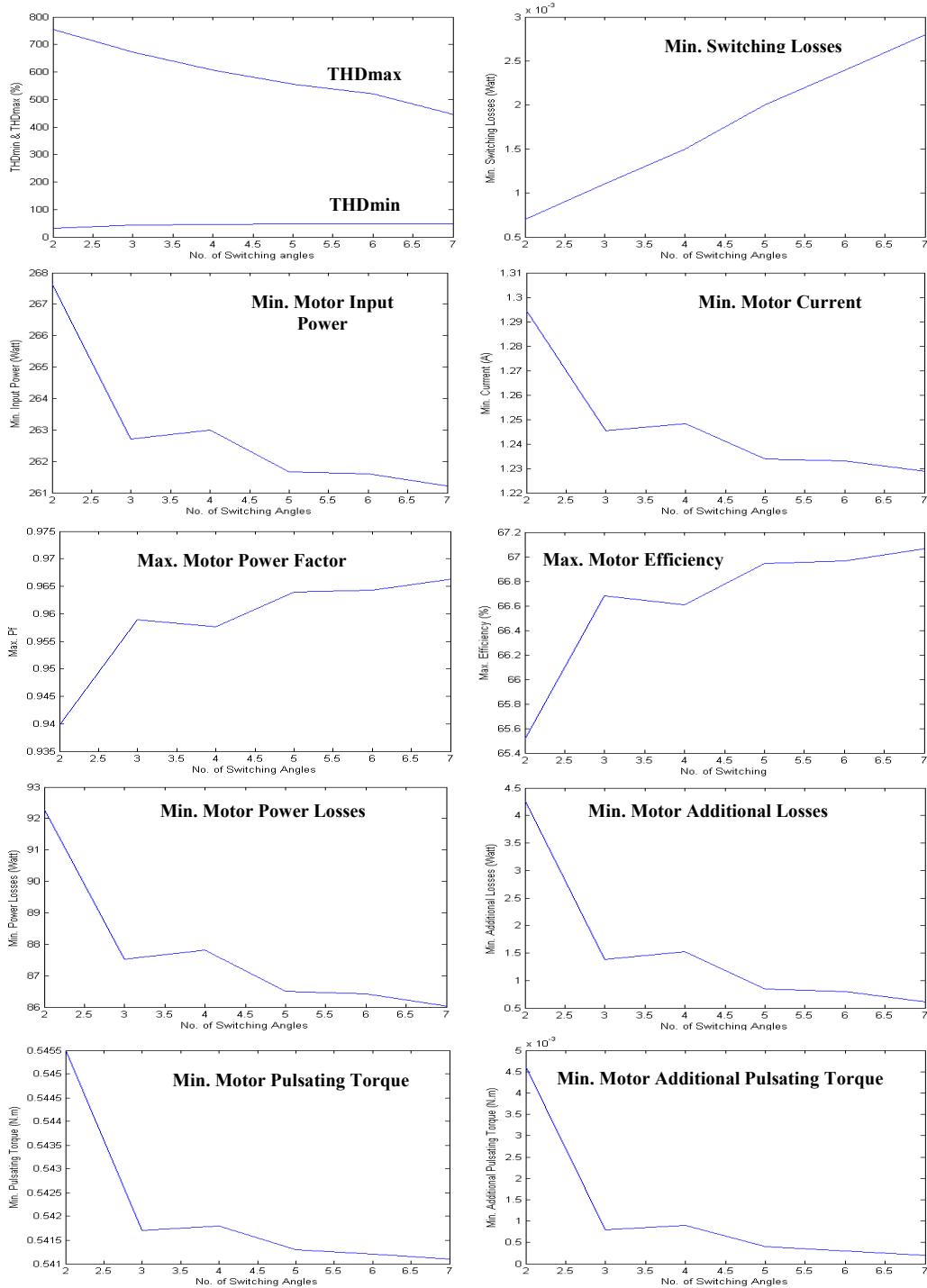


Fig. 8: Optimum Performance of the Inverter and Motor fed from vs. s with Optimal SHPWM Technique

Table 1: the Optimized Performance of SHPWM Inverter and the Proposed Motor Fed from

Switching No. (s)	2	3	4	5	6	7
$\alpha_1$ (Deg)	30.2299	21.8958	22.925	18.8804	18.2243	16.3179
$\alpha_2$ (Deg)	89.7701	36.196	38.2119	28.0493	26.7161	22.7210
$\alpha_3$ (Deg)		45.6422	47.3323	38.182	36.9936	32.9286
$\alpha_4$ (Deg)			89.8262	54.7979	53.1178	45.08
$\alpha_5$ (Deg)				58.2133	56.9332	50.0789
$\alpha_6$ (Deg)					89.9573	66.3199
$\alpha_7$ (Deg)						67.7067
$V_1$ (pu)	0.8600	0.8300	0.8100	0.8000	0.8000	0.7900
$V_3$ (pu)	0	0	0	0	0	0
$V_5$ (pu)	0.1792	0	0	0	0	0
$V_7$ (pu)	0.1177	0.1192	0	0	0	0
$V_9$ (pu)	0	0.0476	0.1642	0	0	0
$V_{11}$ (pu)	0.0847	0.1517	0.1556	0.0338	0	0
$V_{13}$ (pu)	0.0605	0.2166	0.0696	0.1789	0.1520	0
$m$	0.86	0.82	0.81	0.8	0.8	0.79
$THD_{min}$ (%)	31.5599	43.6109	44.6251	47.2747	47.3379	49.1002
$THD_{max}$ (%)	754.8863	671.5544	607.9097	555.3122	521.5931	446.6963
$I_{min}$ (A)	1.2943	1.2453	1.2484	1.2339	1.2331	1.2288
$\eta_{max}$ (%)	65.5167	66.6819	66.6103	66.9442	66.964	67.0636
$P_{fmax}$	0.9398	0.9589	0.9576	0.9639	0.9643	0.9663
$Tpuls_{min}$ (N.m)	0.5455	0.5417	0.5418	0.5413	0.5412	0.5411
$Tpulsadd_{min}$ (N.m)	0.0046	0.0008	0.0009	0.0004	0.0003	0.0002
$\Sigma Padd_{min}$ (W)	4.2568	1.3808	1.5275	0.8425	0.8029	0.6061
$Psw_{min}$ (W)	0.0007	0.0011	0.0015	0.002	0.0024	0.0028
$P_{1min}$ (W)	267.6173	262.7127	262.9976	261.6739	261.596	261.2057
$P_{2min}$ (W)	175.3341	175.1819	175.1836	175.1754	175.1751	175.1739
$\Sigma P_{min}$ (W)	92.2832	87.5307	87.814	86.4985	86.4209	86.0318

Appendix A

$$\begin{aligned}
 \bar{I}_m = \bar{V}_m \frac{ \left[ a_s^2 (R_{1a} + R_f + R_b) \right] + j \left[ X_c + a_s^2 (X_{1a} + X_f + X_b) \right] }{ \left\{ \left[ a_s^2 (R_{1a} + R_f + R_b) \right] + j \left[ X_c + a_s^2 (X_{1a} + X_f + X_b) \right] \right\} } \\
 + ja_s \left[ (R_f - R_b) + j (X_f - X_b) \right] \\
 \frac{ \left[ (R_{1m} + R_f + R_b) + j (X_{1m} + X_f + X_b) \right] - a_s^2 \left[ (R_f - R_b) + j (X_f - X_b) \right]^2 }{ }
 \end{aligned} \tag{A.1}$$

$$\bar{I}_a = \bar{V}_m \frac{\left[ a_s^2 (R_{1m} + R_f + R_b) + j (X_{1a} + X_f + X_b) \right]}{\left\{ \left[ a_s^2 (R_{1a} + R_f + R_b) + j \left[ X_c + a_s^2 (X_{1a} + X_f + X_b) \right] \right] \right\}} \frac{-j a_s \left[ (R_f - R_b) + j (X_f - X_b) \right]}{\left[ (R_{1m} + R_f + R_b) + j (X_{1m} + X_f + X_b) \right] - a_s^2 \left[ (R_f - R_b) + j (X_f - X_b) \right]^2} \quad (A.2)$$

$$\bar{I} = \bar{I}_m + \bar{I}_a \quad (A.3)$$

$$R_f = \frac{X_m^2 R_2 / S}{(R_2 / S)^2 + (x_2 + x_m)^2}, \quad R_b = \frac{X_m^2 R_2 / (2 - S)}{(R_2 / (2 - S))^2 + (x_2 + x_m)^2} \quad (A.4)$$

$$X_f = \frac{X_m \left[ (R_2 / S)^2 + X_2 (X_2 + X_m) \right]}{(R_2 / S)^2 + (x_2 + x_m)^2}, \quad X_b = \frac{X_m \left[ (R_2 / (2 - S))^2 + X_2 (X_2 + X_m) \right]}{(R_2 / (2 - S))^2 + (x_2 + x_m)^2} \quad (A.5)$$

When both windings are connected in parallel,  $V_m = V_a = V_1$ .

The general torque expression for a two phase unbalanced motor is:

$$T_{ins} = \frac{1}{\omega_s} \left\{ \begin{aligned} & I_m^2 \left[ (R_f - R_b) + (R_f - R_b) \cos(2\omega t) - (X_f - X_b) \sin(2\omega t) \right] \\ & + a_s^2 \bar{I}_a^2 \left[ (R_f - R_b) + (R_f - R_b) \cos 2(\varphi + \omega t) - (X_f - X_b) \sin 2(\varphi + \omega t) \right] \\ & + 2 a_s \bar{I}_m \bar{I}_a (R_f + R_b) \sin \varphi \end{aligned} \right\} \quad (A.6)$$

, in which the average torque using the above model is:

$$T_{av} = \frac{1}{\omega_s} \left[ (I_m^2 + a_s^2 \bar{I}_a^2) (R_f - R_b) + 2 a_s (I_m \bar{I}_a \sin \varphi) (R_f + R_b) \right] \quad (A.7)$$

, and the pulsating torque is:

$$T_{puls} = \frac{1}{\omega_s} \left\{ \left[ I_m^4 + (a_s \bar{I}_a)^4 + 2 (a_s I_m \bar{I}_a)^2 \cos(2\varphi) \right] \left[ (R_f - R_b)^2 + (X_f - X_b)^2 \right] \right\}^{1/2} \quad (A.8)$$

The output power, input power and power factor of the motor respectively are:

$$P_2 = T_{av} (1 - S) - W_f \quad (A.9)$$

$$P_1 = \text{Re}(I) V_m + W_i = I V_m \cos(\theta) + W_i \quad (A.10)$$

$$\text{Re}(I) = I \cos \theta \quad [13] \quad (A.11)$$

Table A.1: List of Symbols

Symbol	Parameter	Unit
$\eta, \eta_{max}$	Efficiency and maximum efficiency	%
$I_a, I_m$	Auxiliary-phase and main-phase stator winding currents	A
$I, I_{min}$	Motor line current and minimum line current	A
$\Sigma P_{min}, \Sigma P_{add_{min}}$	Minimum motor power losses and minimum additional power losses	W
$P_f, P_{fmax}$	Motor power factor and maximum power factor	
$P_1, P_2$	Motor input and output power	W
$P_{sw_{min}}$	Minimum switching losses	W
$R_f, R_b$	Effective resistances of stator winding referred to the main-phase forward and backward rotating flux	$\Omega$
$S$	Fractional slip	
$THD_{min}, THD_{max}$	Minimum and Maximum Total Harmonic Distortion	%
$T_{puls_{min}}, T_{puls_{add_{min}}}$	Minimum motor pulsating torque and minimum additional pulsating torque	N.m
$V_a, V_m$	Main-phase and Auxiliary-phase stator winding voltages	V
$V_1$	Supply voltage	V
$W_i, W_f$	Motor iron and friction losses	W
$X_f, X_b$	Effective reactance's of stator winding referred to the main-phase forward and backward rotating flux	$\Omega$
$\theta$	Angle between $I_f$ and $V_m$	Deg
$\varphi$	Phase angle between $I_m$ and $I_a$	Deg

## Appendix B

Table B.1: Parameters and Specifications of the Proposed Motor

Turn ratio	$a_s$	1.066	
Number of pole pair	$P$	2	
Main winding resistance	$R_{1m}$	33.5	$\Omega$
Main winding leakage reactance	$X_{1m}$	27	$\Omega$
Auxiliary winding resistance	$R_{1a}$	34.5	$\Omega$
Auxiliary winding leakage reactance	$X_{1a}$	28	$\Omega$
Rotor resistance	$R_2$	20	$\Omega$
Rotor leakage reactance	$X_2$	12.5	$\Omega$
Magnetization reactance	$X_m$	173	$\Omega$
Rated supply voltage	$V_1$	220	V
Rated current	$I$	1.215	A
Total Power losses	$\Sigma P$	85	W
Input power	$P_1$	260	W
Output power	$P_2$	175	W
Efficiency	$\eta$	67.38	%
Power factor	$P_f$	0.9726	
Rated slip	$S$	0.15	
Rated speed	$N_r$	1275	Rpm
Capacitance	$C$	6	$\mu F$